Angle-resolved Raman spectroscopy of the collective modes in an electron bilayer

D. S. Kainth, D. Richards, A. S. Bhatti,* H. P. Hughes, M. Y. Simmons, E. H. Linfield, and D. A. Ritchie
Cavendish Laboratory, Madingley Road, Cambridge CB3 OHE, United Kingdom
(Received 6 August 1998)

Electronic Raman scattering from GaAs/Al_xGa_{1-x}As double quantum well structures has been used to observe the acoustic and optic plasmon modes of an electron bilayer system. Angle-resolved measurements allowed direct determination of their dispersions for several separations of the electron layers; these were well described by corresponding dispersion calculations in the random-phase approximation (RPA). Qualitative agreement was obtained between measurements of the relative intensities of the acoustic and optic modes and calculations using a simple nonresonant RPA formalism for the Raman scattering cross section. The markedly different linewidths observed for the acoustic and optic modes are interpreted in terms of the greater localization of the electric fields of the acoustic plasmon, which is therefore much less susceptible to impurity damping than is the optic plasmon. [S0163-1829(99)14703-9]

I. INTRODUCTION

Plasmons, the collective oscillatory modes of charged particles, are well known in plasma physics and in studies of the electromagnetic response of solid-state systems. One such collective mode that has attracted considerable interest over the years is the acoustic plasmon (AP—so-called because of its approximately linear dispersion with wave vector), which occurs in systems with two distinct populations of free carriers.[1] These populations can be of different species, such as electrons and holes in a solid[2,3] or electrons and ions in gaseous plasmas,[4] or the two populations of carriers may be separated in momentum space[1,5–7] or real space. For the acoustic mode, similarly charged carriers oscillate out of phase, or oppositely charged carriers oscillate in phase, resulting in the characteristic linear dispersion. When similarly charged carriers oscillate in phase, or oppositely charged carriers oscillate out of phase, the so-called optic plasmon (OP) mode results.

In two-dimensional electron gas (2DEG) systems it is now straightforward to produce samples including two parallel 2DEG's, and these electron bilayers, with distinct populations of carriers separated in real space, are expected to support AP modes. Such modes, which have been extensively studied theoretically,[8–10] have been predicted to enhance the electron-electron interlayer interaction responsible for Coulomb drag between electron sheets,[11–13] and may be involved in mechanisms for high temperature superconductivity.[14–16]

Raman scattering has been extensively used to study electronic excitations in solid state plasmas, but observations of the AP for a two-component semiconductor system have been few. In bulk GaAs Pinzuk *et al.* have reported such a mode in a system with electrons and holes,[2] and more recently Biaramov *et al.* observed the AP in a gas of heavy and light holes.[17] However, in recent years most theoretical attention has been directed toward modulation-doped double quantum well structures containing two spatially separated electron layers.[8,10,18] The dispersions of the various branches of a semiconductor system with conducting multilayers have been determined experimentally,[19–21] and some of these have shown acoustic-like behavior. Acoustic behavior has also been observed in a double quantum well structure with multiple subband occupancy[22] and for a single 2DEG drifting under the effect of an in-plane electric field.[23] However, it is only recently that it has been possible to observe the AP modes in a simple electron bilayer system (i.e., a system comprised of only two distinct populations of carriers, well separated spatially).[24,25]

Here is presented an angle-resolved electronic Raman spectroscopic study of the AP in electron bilayer systems realized in semiconductor double quantum well structures; just one conduction subband in each well is occupied, forming a pair of spatially separated 2DEG's. The interwell separations d are sufficiently large to preclude significant quantum-mechanical interactions, yet small enough to allow direct electromagnetic coupling between charge oscillations in each well. The variety of samples considered has allowed the functional dependence of the plasmon energies and intensities on parameters, such as inter-2DEG separation, spacer layer thickness, and the 2DEG number density, to be explored.

Calculations within the random-phase approximation (RPA) are also reported and shown to model the observed Raman spectra and the dispersive properties of the AP and OP modes quite accurately.

II. EXPERIMENT

The double 2DEG samples studied included two modulation-doped quantum wells separated by an $Al_{0.3}Ga_{0.7}As$ barrier; the well and barrier widths are given in Table I with the 2DEG densities and mobilities determined from 4-K transport measurements in the dark. Samples $A-C$ were grown in a different molecular-beam epitaxy (MBE) chamber from samples D and E, and the two sets of samples differ in several key respects. For samples D and E the widths of the $Al_xGa_{1-x}As$ spacer layers between the doping region and the GaAs quantum wells are 400 Å on the bottom, substrate side, and 200 Å above the top well, whereas for samples $A-C$ the bottom spacer width is 800 Å and the top spacer is 600 Å wide. This results in higher number

 ©1999 The American Physical Society

TABLE I. Quantum well and barrier widths, L_w and L_b, for the samples studied. d is the separation between the well centers and $\hat{d}$ is the distance between the mean positions of the electrons in each well. Number densities N_1, N_2 for the wells were determined by Shubnikov–de Haas measurements without illumination; mobilities μ_1, μ_2 were determined by Hall measurements. The density N_s has been determined from the plasmon dispersion obtained from Raman scattering measurements, as described in the text.

Sample	Wafer	L_w (Å)	L_b (Å)	d $\hat{d}$ (Å)	N_1 N_2 (10^{11} cm^{-2})	μ_1 μ_2 (10^5 cm^2 V^{-1} s^{-1})	N_s (Raman) (10^{11} cm^{-2})
A	*T*223	200	600	800	1.25	2.2	1.97±0.10
				829	1.3	2.0	
B	*T*225	150	300	450	1.8	1.1	2.10±0.10
				462	1.8	1.1	
C	*T*229	180	125	305	1.35	1.4	1.95±0.10
				326	1.2	1.4	
D	*A*994	200	600	800	2.1	0.97	3.8±0.2
					3.6	0.74	
E	*C*779	200	300	500	2.2	0.89	3.4±0.5
					3.4	0.11	

densities N_1, N_2 in the two quantum wells for samples *D* and *E* but a lower mobility due to enhanced Coulombic scattering between the electrons in the 2DEG's and the remote ionized donors. Samples *D* and *E* also have an n^+ backgate.[26] Samples *A*–*C* were used for the work reported in Ref. 25 and a preliminary report of Raman measurements from sample *E* was given in Ref. 24.

For each sample, self-consistent Poisson-Schrödinger calculations were made for the conduction-band profile and the probability density function $[|\psi(z)|^2]$ of the single electron wave functions, and the results for sample *C* are shown in Fig. 1. For all samples, the interwell barrier width L_b is sufficiently large to preclude significant quantum-mechanical interactions (as is evident from the calculated envelope wave functions) but allows direct electromagnetic coupling between charge oscillations in each well. Each of the wells is expected to support only one occupied subband, with the energy gap between the first and subsequent subbands large compared to the Fermi energy (see Fig. 1).

In samples *A*–*C* the calculations also revealed the (unintentional) possibility of a third 2DEG buried deep within the heterostructure ($\sim$0.6 μm below the lower quantum well). The $Al_xGa_{1-x}As$ layer is graded on the substrate side in an attempt to ensure that such a 2DEG does not form at this heterointerface, but our measurements did suggest its existence in sample *A*. However, its distance from the active region (any interactions with the double quantum well structure will be Coulombic) and its low number density ensure that its effects can be safely disregarded in any subsequent analysis.

Many calculations of electron bilayer systems assume that the 2DEG's can be modeled as sheets of charge of a given separation; it is convenient to define inter-2DEG separations *d*, the distance between the centers of the two quantum wells, and $\hat{d}$, the distance between the mean of the electron distributions $[|\psi(z)|^2]$. The values of *d* are given in Table I, where $\hat{d}$ is also given for samples *A*–*C*.

A backscattering Raman geometry was employed, so the wave-vector transfer parallel to the semiconductor layers could be varied continuously by rotating the sample about an axis perpendicular to the growth direction.[27] Samples were held on the cold finger of a liquid-He bath cryostat, in an atmosphere of He gas, at a temperature of 8 K. The incident power density was 40 W cm^{-2}, which results in heating of the electron gas to about 25 K (see Ref. 28 for further details about temperature dependence). Scattered light was spectrally analyzed with a triple grating spectrometer and detected with an intensified multichannel diode array. Raman spectra were measured with the incident and scattered polarizations parallel; for this polarization configuration, Raman scattering by charge-density excitations (plasmons) is selection-rule allowed.[29]

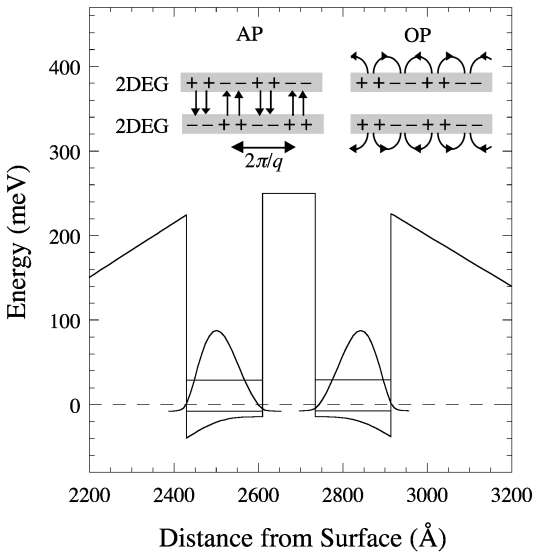

FIG. 1. Electrostatic potential and probability densities $|\psi(z)|^2$ for the occupied subbands of sample *C*. The energy levels for the first two subbands in each quantum well are also indicated; the dashed line corresponds to the position of the Fermi energy. The inset shows a representation of the acoustic (AP) and optic (OP) plasmons of wave vector *q*; the arrows indicate the main contributions to the electric fields for the two modes and +(−) indicates a depletion (accumulation) of electrons.

III. BACKGROUND THEORY

A semiquantitative understanding of the behavior of the plasmon modes in an electron bilayer can be obtained from purely classical arguments. If the areal number densities of the upper and lower 2DEG's are N_1 and N_2, the dispersion relation for the two plasmon modes in the bilayer obtained from classical electrodynamics is

$$\omega^2_{(\substack{AP\\OP})} = \frac{e^2 q}{2\epsilon\epsilon_0 m^*}(N_1+N_2) \times\left[\frac{1}{2}\mp\frac{1}{2}\sqrt{1-\frac{4N_1N_2}{(N_1+N_2)^2}(1-e^{-2qd})}\right], \quad (1)$$

where ω is the mode frequency at wave vector q, ϵ is the effective background dielectric constant, d is the effective separation between the two 2DEG's (as discussed above), and m^* is the electron effective mass. This equation, although not quantitatively exact, gives a good physical insight into the behavior of the modes and how this depends on various sample parameters. The $+$ sign corresponds to the charge-density oscillations in each layer being in phase; this OP mode resembles that for a single electron gas layer and disperses $\sim q^{1/2}$ for $qd \ll 1$. The $-$ sign corresponds to the oscillations being out of phase, as for the AP mode, and the dispersion $\sim q$ for $qd \ll 1$. A schematic representation of the two plasmons is shown in the inset of Fig. 1.

In order to obtain a more reliable comparison between experiment and theory, the plasmon dispersions were determined within the Singwi-Tosi-Land-Sjölander (STLS) extension of the random-phase approximation (RPA) for $T=0$ K.[18,28] For the wave-vector range considered here $q \leqslant 0.15k_F$ (where k_F is the Fermi wave vector), exchange-correlation corrections, incorporated within the STLS, are in fact small and the form of the plasmon dispersion is essentially just that given by the RPA. The quantum well subbands were assumed to disperse parabolically, and the intralayer and interlayer Coulomb matrix elements were calculated using envelope wave functions $\psi(z)$ (e.g., see Fig. 1) determined self-consistently from the Poisson and Schrödinger equations.[21] Interactions between phonons and the collective electronic modes were included by using a frequency-dependent background dielectric function,

$$\epsilon(\omega) = \epsilon(\infty)\left(\frac{\omega^2-\omega_{LO}^2}{\omega^2-\omega_{TO}^2}\right). \quad (2)$$

Raman scattering line shapes $R(q,\omega)$ were determined within the RPA:[30]

$$R(q,\omega) \propto -\int dz \int dz' \left[\sum_{ij} \mathrm{Im}[\chi_{ij}(q,\omega)] \times |\psi_i(z)|^2 |\psi_j(z')|^2\right] e^{-2ik_L(z-z')} e^{-(z+z')/\delta}, \quad (3)$$

where $\chi_{ij}(q,\omega)$ are the elements of the RPA bilayer density response function $\overline{\overline{\chi}}(q,\omega)$ (Ref. 28) and $\psi_i(z)$ is the envelope wave function in layer i. k_L and δ are the wave vector and decay length of the light in the semiconductor. Although such an approach does not take into account the effects of resonance in the Raman scattering process, it has nevertheless been shown to provide a good description of electronic Raman spectra.[29]

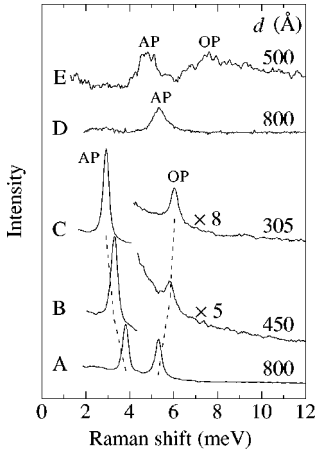

FIG. 2. Low-temperature Raman spectra for all the samples, measured at an incoming resonance, with an in-plane wave-vector transfer $q=1.35\times10^5$ cm^{-1} for samples A–D, and $q=1.42\times10^5$ cm^{-1} for sample E. Samples D and E have higher electron densities than samples A–C (see Table I).

IV. RESULTS

Figure 2 shows polarized Raman spectra for all five samples, taken with an in-plane wave-vector transfer of $q=1.35\times10^5$ cm^{-1} for samples A–D and $q=1.42\times10^5$ cm^{-1} for sample E. Two peaks are observed in the spectra for samples A–C (less clearly for samples D and E); we ascribe the lower-energy mode to the AP and the upper-energy mode to the OP.

Raman scattering by both plasmons was found to be strongly resonant in all five samples. Figure 3 shows a set of spectra for sample C with varying incident excitation energy. In the lowest two spectra a broad peak (PL) due to hot photoluminescence from a high-lying subband of the quantum well structure is observed. The OP mode clearly comes into an outgoing resonance with this interband transition for a laser energy of $\sim$1.662 eV. For all the samples no signals corresponding to spin-density and single-particle spin-flip excitations were observed with incident and scattered polarizations orthogonal. For the intermediate values of q used here, the intrasubband single-particle excitation (SPE) band potentially observable in the polarized Raman spectra[27,29,31] was in a spectral region too close (a Raman shift less than 10 cm^{-1}) to the exciting laser line to be observed.

V. PLASMON DISPERSIONS

There are a number of important differences between the Raman spectra for samples A–C and those for samples D and E, evident in Fig. 2, which will be discussed later; for the moment the discussion will be restricted to the high-mobility samples A–C. Figure 4 shows low-energy polarized Raman spectra for sample C for various in-plane wave-vector trans-

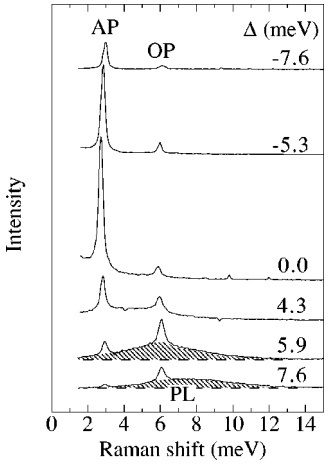

FIG. 3. Raman spectra for sample *C* as a function of the detuning $\Delta\ (=E_L-\Omega_0)$ of the incident laser energy E_L from the resonance energy $\Omega_0=1.656$ eV. Note the outgoing resonance for the optic plasmon for $\Delta=6$ meV. The hot photoluminescence feature (PL) results from the interband transition responsible for the resonance.

fers *q*, taken at a lattice temperature of 7 K and an excitation energy of 1.656 eV; a similar set of spectra for sample *A*, obtained with an excitation energy of 1.623 eV, are shown in Fig. 5. In both cases the two plasmon peaks clearly disperse with *q*. Figure 6 shows the measured dispersions for the OP and AP modes for samples *A* and *C* out to $q\sim1.6\times10^5$ cm^{-1} ($\sim0.15k_F$, the Fermi wave vector for the sample areal 2DEG densities N_1 and N_2 determined below).

The solid lines in Fig. 6 represent fits to the data, using the RPA approach outlined in Sec. III, using the electron number densities in the two wells, N_1 and N_2, as fitting parameters. Because of the insensitivity of the fits to the relative values of N_1 and N_2 for a given total density N_1+N_2, N_1 and N_2 were both set equal (to N_s), and the values of N_s determined in this way for all five samples are given in Table I. (The individual values of N_1 and N_2 were estimated to be within 5% of N_s and the total density N_1+N_2 within 1% of $2N_s$.) These are larger than those obtained from

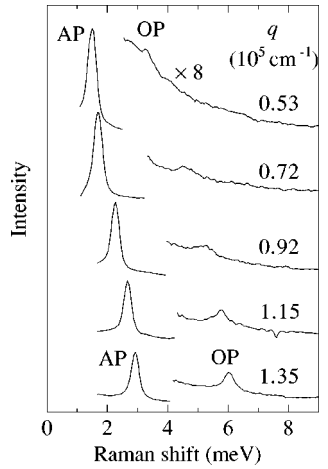

FIG. 4. Raman spectra for sample *C* for different in-plane wave vectors *q*, measured with an excitation energy of 1.656 eV. The OP produces a much weaker signal than the AP for this particular value of *d*.

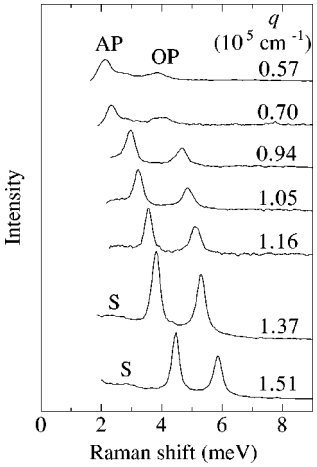

FIG. 5. Raman spectra for sample *A* for different in-plane wave vectors *q*, measured with an excitation energy of 1.623 eV. The weak low-energy feature *S* may be due to a plasmon in a low-density 2DEG buried deep within the heterostructure.

Shubnikov–de Haas measurements in the dark because of the different illumination conditions (see Table I); they are, however, consistent with the Fermi energy E_F determined from the width of the quantum well PL.

So, under illumination the number densities for the three samples *A*–*C* were roughly equivalent, and the principal difference was thus the inter-2DEG separation, *d*. As expected from simple theory [Eq. (1)], the energy separation between the two modes increases as *d* decreases (Fig. 2 and Fig. 6). The effect of the electron density on the plasmon energy can also be readily seen from a comparison of the Raman spectra for samples *A* and *D* in Fig. 2. The quantum well and barrier widths are the same for these two structures but the density in sample *D* is twice that in sample *A*, resulting in the 40% increase in the AP energy.

A weak dispersing feature (*S*) is also present in the high-wave-vector spectra for sample *A* (see Fig. 5), which can be ascribed to a plasmon in an electron gas of density $\sim6\times10^{10}$ cm^{-2} at the inverted heterointerface deep within the

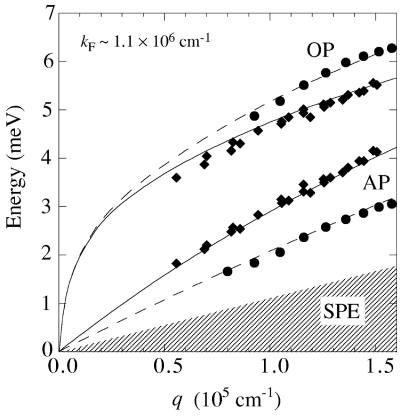

FIG. 6. Dispersion of the optic (OP) and acoustic (AP) plasmon modes for samples *A*(♦) and *C* (●). The curves are calculated using the zero-temperature RPA with an STLS correction, and with values of $N_1=N_2=N_s$ chosen to optimize the fit to the data (see text and Table I). The shaded region shows the continuum of single particle transitions expected for these number densities.

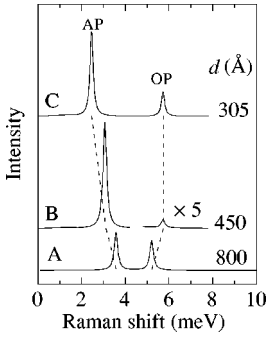

FIG. 7. Theoretical Raman spectra for samples $A-C$ (i.e., as a function of electron layer separation d).

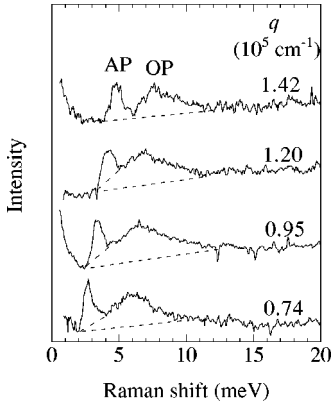

FIG. 8. Raman spectra for sample E, obtained with an excitation energy of 1.705 eV, showing the dispersions of the AP and OP. The OP is significantly broader than that of the AP, ascribed to a partial breakdown of wave-vector conservation due to enhanced dopant scattering.

structure. The distance between this 2DEG and the electron bilayer is sufficiently large, and the difference in densities sufficiently great, to preclude any significant interaction between the plasmons in the two electron systems.

VI. RAMAN SCATTERING INTENSITIES

The ratio of the AP and OP Raman intensities has been predicted to be strongly dependent on the laser wavelength in the semiconductor and on d.[30] This can be understood in terms of interference between the scattered light from the two 2DEG's; in the simple case of the true backscattering geometry in which k_L, the light wave vector in the semiconductor, is assumed to be normal to the 2DEG planes, for the in-phase OP, Raman scattering by charge-density fluctuations will be a maximum when $k_L d = n\pi$, whereas the maximum intensity will occur for the out-of-phase fluctuations associated with the AP when $k_L d = (n+\frac{1}{2})\pi$ (n is an integer). For the experiments presented here, the wavelength $2\pi/k_L \approx 2000$ Å, and it is clear from Fig. 2, and from a comparison of Figs. 4 and 5, that there is a strong dependence of the relative strengths of the optic and acoustic plasmons on the layer separation d for samples $A-C$. Calculations of the Raman cross section, in which the interference effect described above is taken into account by the $e^{-2ik_L(z-z')}$ term in Eq. (3), indicate that the effect of this interference on the Raman intensities of the two plasmon modes is far more significant than that of reduced electromagnetic coupling between layers on increasing the bilayer separation d. Figures 4 and 5 also show that the OP gains strength compared with the AP with increasing wave vector q, in line with the predictions of Ref. 30.

The experimental spectra for samples $A-C$ in Fig. 2 can be compared with those obtained in the RPA calculation [Eq. (3)], shown in Fig. 7 (the plasmon energies are slightly higher than those obtained within the STLS approach, used to determine the 2DEG densities). For $q = 1.35\times10^5$ cm^{-1} the experimental intensity ratios (AP to OP) are 1.2 (sample A), 18 (sample B), and 24 (sample C), and the RPA calculations give 1.3 (sample A), 58 (sample B), and 3.3 (sample C). There is a semiquantitative agreement between experiment and theory, particularly for samples A and B. The excitation energies used here were chosen to give an incoming resonance for each sample, under the premise that both the AP and OP would be similarly resonantly enhanced. The discrepancies between experiment and theory for the AP/OP intensity ratios can probably be ascribed to different resonant enhancements of the two modes, not included in this nonresonant Raman scattering model.[29] Difficulties in tuning the laser energy exactly to the incoming resonance, and on 5% uncertainties in the well widths will also be factors. In addition, in our calculation we have determined the wavelength of light in the semiconductor ($\sim$2000 Å) using a refractive index of 3.7; we have not taken into account the effect of the variation in refractive index with composition across the heterostructure. However, bearing in mind these limitations, the good agreement obtained indicates the power of modeling resonant electronic Raman scattering line shapes using simple linear-response theory.

VII. EFFECTS OF SAMPLE QUALITY

The AP and OP for the lower mobility samples D and E were found to disperse as expected (see, e.g., Fig. 8 and Ref. 24 for sample E), but with the plasmons at higher energies compared to those for samples $A-C$ because of the higher densities in these samples (see Table I). However, comparing the Raman spectra for the two sets of samples (Fig. 2), it can be seen that, whereas the two plasmon peaks are of comparable width for samples $A-C$, for sample E the width of the OP is significantly broader than that of the AP and for sample D the OP was not observed, despite an extensive search for suitably resonant conditions (an RPA calculation predicts the AP and OP intensities to be comparable for sample D, cf. sample A). In addition, although sample E displayed a number of resonances for the AP, the OP was observed only for an incident energy of 1.705 eV.

The lower mobilities of samples D and E indicate shorter single-particle lifetimes for these two samples, which will result in an increased damping of the plasmons, and indeed the AP Raman peak for samples D and E is clearly broader than that for samples $A-C$. However, increased single-particle scattering should affect both the AP and OP modes equally and so cannot account for the significant broadening of the OP peak compared to that of the AP. This effect must be associated with scattering of the plasmons themselves, leading to a partial breakdown of wave-vector conservation

in the Raman scattering process for the OP—wave-vector conservation breakdown has been invoked to explain Raman scattering by high-wave-vector modes in the integer and fractional quantum Hall regimes.[32–34]

The charge oscillations in each 2DEG are out of phase for the AP, so the electromagnetic fields associated with the AP are strongly localized between the active layers.[21] However, the in-phase charge oscillations of the OP result in much larger fields in the regions outside the double well structure, than for the AP,[21] resulting in an enhancement of the scattering interaction of the OP with mobile carriers in the doped $Al_xGa_{1-x}As$ layers (and possibly with the n^+-type GaAs back gate). The plasmon fields decay exponentially with distance from the 2DEG's (Ref. 21) and so this interaction is likely to be much more significant for samples *D* and *E*, which have much thinner spacer layers than samples *A*–*C*, leading to scattering of the OP and hence a partial loss of wave-vector conservation, resulting in the broad, or non- existent, OP feature for these samples. However, it should be noted that there cannot be complete relaxation of wave-vector conservation for the OP, since this mode disperses with q as expected[24] (Fig. 8).

The high integrated intensity of the OP mode in Fig. 8 (sample *E*) compared to that of the AP mode is also a surprise, since for the excitation wavelength (727 nm) used for these measurements and the layer separation d, Raman scattering by the AP is expected to be much stronger than that for the OP (cf. sample *B*). The fact that this mode was observed only over a narrow range of excitation energies, whereas a number of Raman resonances were observed for the AP, indicates a very strong resonant enhancement for this non-wave-vector conserving process.

VIII. SUMMARY

The acoustic plasmon in a two-component system has been successfully observed using Raman spectroscopy to probe an MBE-grown conducting double layer system containing just two 2DEG's, separated spatially so that tunneling between the electron layers is not possible but allowing strong Coulomb interactions. Good agreement was obtained between experiment and RPA theory for the plasmon dispersions, using the electron density as a fitting parameter. The Raman spectra, although measured under resonant conditions, are described well using the dielectric response determined within the RPA. Because of its more extensive field distribution, the optic plasmon was much more sensitive than the acoustic plasmon to scattering processes associated with the layers surrounding the electron bilayer, leading to a partial loss of wave-vector conservation in the Raman scattering process for samples with thin spacer layers between the quantum wells and the dopant layers.

ACKNOWLEDGMENTS

We thank the U.K. Engineering and Physical Sciences Research Council and the Royal Society for support.

*Present address: Department of Physics, University of the Punjab, Lahore-54590, Pakistan.

[1] P. M. Platzman and P. A. Wolff, *Waves and Interactions in Solid State Plasmas* (Academic Press, New York, 1973).
[2] A. Pinczuk, J. Shah, and P. A. Wolff, Phys. Rev. Lett. **47**, 1487 (1981).
[3] D. C. Scott, R. Binder, and S. W. Koch, Phys. Rev. Lett. **69**, 347 (1992).
[4] See e.g., L. Tonks and I. Langmuir, Phys. Rev. **33**, 195 (1929).
[5] D. C. Scott, R. Binder, M. Bonitz, and S. W. Koch, Phys. Rev. B **49**, 2174 (1994).
[6] K. El Sayed, R. Binder, D. C. Scott, and S. W. Koch, Phys. Rev. B **47**, 10 210 (1993).
[7] K. Kempa, P. Bakshi, J. Cen, and H. Xie, Phys. Rev. B **43**, 9273 (1991).
[8] S. Das Sarma and A. Madhukar, Phys. Rev. B **23**, 805 (1981).
[9] R. Z. Vitlina and A. V. Chaplik, Zh. Éksp. Teor. Fiz. **81**, 1011 (1981) [Sov. Phys. JETP **54**, 536 (1981)].
[10] G. E. Santoro and G. F. Giuliani, Phys. Rev. B **37**, 937 (1988).
[11] K. Flensberg and B. Y.-K. Hu, Phys. Rev. Lett. **73**, 3572 (1994).
[12] K. Flensberg and B. Y.-K. Hu, Phys. Rev. B **52**, 14 796 (1995).
[13] N. P. R. Hill, J. T. Nicholls, E. H. Linfield, M. Pepper, D. A. Ritchie, G. A. C. Jones, B. Y.-K. Hu, and K. Flensberg, Phys. Rev. Lett. **78**, 2204 (1997).
[14] J. Rüvalds, Phys. Rev. B **35**, 8869 (1987).
[15] Y. Ishii and J. Rüvalds, Phys. Rev. B **48**, 3455 (1993).
[16] S.-M. Cui and C.-H. Tsai, Phys. Rev. B **44**, 12 500 (1991).
[17] B. Kh. Bairamov, V. A. Voitenko, I. P. Ipatova, V. K. Negoduyko, and V. V. Toporov, Fiz. Tekh. Poluprovdn. **28**, 913 (1994) [Semiconductors **28**, 531 (1994)].
[18] L. Liu, L. Swierkowski, D. Neilson, and J. Szymanski, Phys. Rev. B **53**, 7923 (1996).
[19] A. Pinczuk, M. G. Lamont, and A. C. Gossard, Phys. Rev. Lett. **56**, 2092 (1986).
[20] G. Fasol, N. Mestres, H. P. Hughes, A. Fischer, and K. Ploog, Phys. Rev. Lett. **56**, 2517 (1986).
[21] G. Fasol, R. D. King-Smith, D. Richards, U. Ekenberg, N. Mestres, and K. Ploog, Phys. Rev. B **39**, 12 695 (1989).
[22] D. Richards, G. Fasol, and K. Ploog, Appl. Phys. Lett. **56**, 1649 (1990).
[23] A. S. Bhatti, D. Richards, H. P. Hughes, and D. A. Ritchie, Phys. Rev. B **53**, 11 016 (1996).
[24] A. S. Bhatti, D. Richards, H. P. Hughes, E. H. Linfield, D. A. Ritchie, and G. A. C. Jones, in *Proceedings of the 23rd International Conference on the Physics of Semiconductors*, edited by M. Scheffler and R. Zimmermann (World Scientific, Singapore, 1996), p. 1899.
[25] D. S. Kainth, D. Richards, H. P. Hughes, M. Y. Simmons, and D. A. Ritchie, Phys. Rev. B **57**, R2065 (1998).
[26] K. M. Brown, E. H. Linfield, D. A. Ritchie, G. A. C. Jones, M. P. Grimshaw, and A. C. Churchill, J. Vac. Sci. Technol. B **12**, 1293 (1994).
[27] A. Pinczuk and G. Abstreiter, in *Light Scattering in Solids V*, edited by M. Cardona and G. Güntherodt (Springer, Heidelberg, 1988), p. 153.
[28] D. S. Kainth, D. Richards, H. P. Hughes, M. Y. Simmons, and D. A. Ritchie (unpublished).
[29] G. Abstreiter, M. Cardona, and A. Pinczuk, in *Light Scattering in Solids IV*, edited by M. Cardona and G. Güntherodt (Springer, Heidelberg, 1984) p. 5.
[30] G. E. Santoro and G. F. Giuliani, Phys. Rev. B **37**, 8443 (1988).

[31] D. Richards, B. Jusserand, H. Peric, and B. Etienne, Phys. Rev. B **47**, 16 028 (1993).

[32] A. Pinczuk, J. P. Valladares, D. Heiman, A. C. Gossard, J. H. English, C. W. Tu, L. Pfeiffer, and K. West, Phys. Rev. Lett. **61**, 2701 (1988).

[33] I. K. Marmorkos and S. Das Sarma, Phys. Rev. B **45**, 13 396 (1992).

[34] H. D. M. Davies, J. C. Harris, J. F. Ryan, and A. J. Turberfield, Phys. Rev. Lett. **78**, 4095 (1997).